

Pressure effects on an $S=1/2$ Heisenberg two-leg ladder antiferromagnet $\text{Cu}_2(\text{C}_5\text{H}_{12}\text{N}_2)_2\text{Cl}_4$

メタデータ	言語: eng 出版者: 公開日: 2007-11-19 キーワード (Ja): キーワード (En): 作成者: Mito, M, Akama, H, Kawae, T, Takeda, K, Deguchi, H, Takagi, S メールアドレス: 所属:
URL	http://hdl.handle.net/10228/359

Pressure effects on an $S = \frac{1}{2}$ Heisenberg two-leg ladder antiferromagnet $\text{Cu}_2(\text{C}_5\text{H}_{12}\text{N}_2)_2\text{Cl}_4$

M. Mito, H. Akama, T. Kawae, and K. Takeda

Department of Applied Quantum Physics, Faculty of Engineering, Kyushu University, Fukuoka 812-8581, Japan

H. Deguchi and S. Takagi

Faculty of Engineering, Kyushu Institute of Technology, Kitakyushu 804-8550, Japan

(Received 17 August 2001; published 7 February 2002)

The pressure effects on an $S = 1/2$ Heisenberg two-leg ladder antiferromagnet (H2LLAF) $\text{Cu}_2(\text{C}_5\text{H}_{12}\text{N}_2)_2\text{Cl}_4$ have been investigated through magnetic and thermal measurements under pressures up to 10 kbar. The exchange interactions along the rung and leg hardly change under pressures, but the pressurization induces paramagnetic spins and magnetic order. This magnetic order is a pressure-induced one observed in a quantum spin system with an energy gap. The amount of induced paramagnetic spins increases almost in accordance with the square of pressure. The magnetic field dependence of the pressure-induced Schottky-type heat capacity suggests that the induced paramagnetic spins are not completely free, but weakly correlate with the H2LLAF system. A magnetic anomaly of the heat capacity has been observed around 2.6 K for $P \geq 8.5$ kbar, where more than 20% of the paramagnetic spins are induced. This anomaly is considered to be intrinsic to the magnetic order of the H2LLAF system, which seems to be triggered by the modulation of the staggered moment due to local defects. Even below the magnetic ordering temperature, the paramagnetic spins coexist with the magnetic order of the H2LLAF system. These pressure effects are similar to the impurity effects in another typical $S = 1/2$ H2LLAF SrCu_2O_3 doped with nonmagnetic Zn^{2+} ions.

DOI: 10.1103/PhysRevB.65.104405

PACS number(s): 75.50.Ee, 75.40.Cx, 81.40.Vw, 75.10.Jm

I. INTRODUCTION

Low-dimensional Heisenberg antiferromagnetic (HAF) systems show a variety of quantum effects such as the Haldane gap¹ and the spin Peierls transition.² Isotropic one-dimensional (1D) and two-dimensional (2D) HAF quantum spin systems with $S = 1/2$ have continuous eigenstates above the ground state. The ladder system, which is an intermediate system between 1D and 2D ones, from a crystallographical point of view, has a quantum coherent state with an energy gap (Δ) above the ground state at low temperatures.³⁻¹⁷ This gap originates from the strong intradimer and small interdimer couplings. The Hamiltonian of the $S = 1/2$ Heisenberg two-leg ladder antiferromagnet (H2LLAF) is expressed as

$$\mathcal{H} = -J_{\perp} \sum_i^{N/2} \mathbf{S}_{1,i} \cdot \mathbf{S}_{2,i} - J_{\parallel} \sum_i^{N/2} (\mathbf{S}_{1,i} \cdot \mathbf{S}_{1,i+1} + \mathbf{S}_{2,i} \cdot \mathbf{S}_{2,i+1}), \quad (1)$$

where J_{\perp} and J_{\parallel} denote, respectively, the interactions along the rung and leg, $\mathbf{S}_{n,i}$ is the Heisenberg type of spin operator with spin value $1/2$, and N represents the total number of spins. The magnitude of the gap is approximated as $\Delta \approx |J_{\perp} - J_{\parallel}|$.¹⁰ The two-leg ladder has an energy gap, while the three-leg one does not. The compounds SrCu_2O_3 (Refs. 3-5) and $\text{Cu}_2(\text{C}_5\text{H}_{12}\text{N}_2)_2\text{Cl}_4$ (CuHpCl) (Refs. 6-17) have been recognized as representative compounds of the $S = 1/2$ H2LLAF systems.

SrCu_2O_3 has a large energy gap $\Delta/k_B = 420$ K, and its magnetism has been intensively investigated.^{3,4} In the Zn-doped system $\text{Sr}(\text{Cu}_{1-x}\text{Zn}_x)_2\text{O}_3$, an increase of the paramagnetic susceptibility with increasing x has been observed and, furthermore, antiferromagnetic order has been detected in systems of $0.01 < x < 0.08$.⁵ Fukuyama *et al.* have ex-

plained that this ordering is triggered by the modulation of the staggered moment induced by the local randomness.¹⁸

The gap in CuHpCl is relatively small ($\Delta/k_B = 10.5$ K), and magnetic properties of the compounds, especially under magnetic fields, have been studied through various experiments such as magnetic susceptibility,^{7,8,10,13,14} magnetization,^{7,8,10,13,14} heat capacity,^{7,10,16,17} NMR,^{9,11,12} electron spin resonance (ESR),¹³⁻¹⁵ and neutron scattering measurements.¹⁰ From these experiments, the values of the exchange interactions and the critical field (H_c) for quenching the energy gap have been estimated as $J_{\perp}/k_B = -13.2$ K, $J_{\parallel}/k_B = -2.4$ K, and $H_c = 7.5$ T, respectively. Furthermore, through the thermal measurements in the external magnetic field H above 9 T ($> H_c$), field-induced magnetic ordering has been observed around 0.7 K.^{10,16,17} Corresponding to these experimental results (Refs. 10, 16, and 17), some theoretical studies of the thermodynamic properties under magnetic fields have been also reported.^{19,20}

Motivated by the above studies of CuHpCl under magnetic fields, we have been interested in the pressure effects on J_{\perp} , J_{\parallel} , and Δ in CuHpCl. We anticipated the following phenomena: Pressurization might induce anisotropic intermolecular shrinkage, which would change $\Delta \approx |J_{\perp} - J_{\parallel}|$. The quenching of Δ by pressurization would induce magnetic ordering due to interladder interactions at zero magnetic field. In this paper, we report the pressure effects on the $S = 1/2$ H2LLAF CuHpCl through magnetic and thermal measurements under pressures up to 10 kbar. The experimental results indicate that the pressure (1) hardly changes J_{\perp} and J_{\parallel} and (2) induces paramagnetic moments and magnetic ordering. As for the quantum spin system with an energy gap, field-induced magnetic order has been already observed in some compounds such as CuHpCl (Refs. 10, 16, and 17) and the Haldane compounds,^{21,22} but the pressure-induced one is

presented in this paper. These effects of pressure on CuHpCl are very similar to impurity effects on SrCu₂O₃ doped with nonmagnetic Zn²⁺ ions.

Explanations about the sample and experimental apparatus will be given in Sec. II. In Sec. III, the experimental results will be shown and analyzed. In Sec. IV, a model will be proposed in order to explain the experimental results.

II. EXPERIMENTS

The preparation of Cu₂(C₅H₁₂N₂)₂Cl₄ has been followed by a procedure described elsewhere.⁶ This compound crystallizes in the monoclinic space group $P2_1/c$, and the lattice parameters at room temperature are $a = 13.406(3)$ Å, $b = 11.454(2)$ Å, $c = 12.605(3)$ Å, and $\beta = 115.01(2)^\circ$.⁶ The copper binuclear unit forming the dimer stacks up along the [101] direction. The dimers form an infinite ladder structure through the hydrogen bond of Cu-Cl-H-N-Cu along the [101] direction. The intradimer Cu-Cu distance is 3.422 Å, and the interdimer distance along the chains is 7.00 Å. The adjacent ladders are held together by van der Waals forces, and the distance between two adjacent ladders exceeds 8 Å. The interladder interaction is expected to be weak.

The pressure was produced by two types of CuBe clamp cells with the following inner and outer diameters: 3–7 mm for the magnetic²³ and 6–12 mm for the thermal^{24,25} measurements. As the pressure transmitting medium, fluorine oil was used for the magnetic and Apiezon-J grease for the thermal measurements. Prior to this experiment, the relation between the load at room temperature and the pressure at low temperatures was calibrated through the change of the superconducting transition of metallic Pb by pressurization.²⁶

The magnetization (M) curve against the magnetic field $H \leq 5$ T at temperature $T = 1.7$ K and dc magnetic susceptibility ($\chi = M/H$, $H = 0.1$ T, and 1.8 K $\leq T \leq 100$ K) were measured with a superconducting quantum interference device (SQUID) magnetometer (Quantum Design MPMS-5S) in the pressure region up to 8 kbar. A powder sample of 128.0 mg was used for this magnetic measurement.

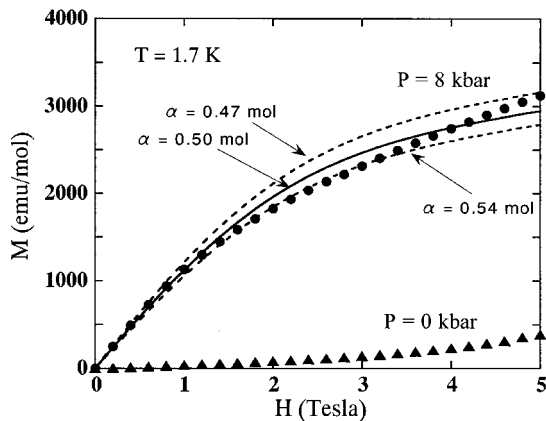


FIG. 1. Magnetization (M) vs the magnetic field (H) of CuHpCl at $T = 1.7$ K for $P = 0$ and 8 kbar. The solid and dotted curves show data retrieved from Eq. (2) with $S = 1/2$, $g = 2.08$, and $\alpha = 0.47$ – 0.54 mol.

The heat capacity was measured with the adiabatic heat-pulse method in the temperature region from 0.8 to 10 K. The samples of CuHpCl (646.9 mg) and Apiezon-J grease (233.6 mg) were mixed well to accelerate the thermal relaxation. The magnetic heat capacity (C_p) of CuHpCl was derived, taking the pressure effects on the heat capacity of Apiezon-J grease and the lattice heat capacity of CuHpCl into consideration.²⁴ The lattice heat capacity at each pressure was estimated by the Debye function adjusted so the total magnetic entropy for $S = 1/2$ was preserved.

At pressure $P = 9.7$ kbar, which is the maximum pressure in the present series of experiments, the real part of the ac susceptibility (χ') was also measured simultaneously with the heat capacity by use of an ac bridge (the ac field $H_{ac} = 0.1$ Oe peak-to-peak and the frequency $f = 15.9$ Hz).

III. EXPERIMENTAL RESULTS AND ANALYSIS

A. Magnetic measurement

Figure 1 shows the magnetization (M) curve up to $H = 5$ T at $T = 1.7$ K for $P = 0$ and 8 kbar. At ambient pressure ($P = 0$ kbar), the development of M in the magnetic field region $H \leq 5$ T is suppressed by the existence of the energy gap $\Delta/g\mu_B = 7.5$ T. It is noted, however, that the result for M at $P = 8$ kbar shows the paramagnetic contribution without any behavior typical for the gap system.^{8,14}

For simplicity, we analyze the result for M at $P = 8$ kbar as the summation of the H2LLAF contribution and the paramagnetic one with the Brillouin function (B_S):

$$M(P = 8 \text{ kbar}) = \alpha M(P = 0 \text{ kbar}) + (1 - \alpha)Ng\mu_B S B_S(gS\mu_B H/k_B T), \quad (2)$$

where N is the Avogadro number, μ_B the Bohr magneton, g Lande's g factor, k_B the Boltzmann factor, and α ($0 \leq \alpha \leq 1$) the amount of the spins in the H2LLAF system. Here the change of J_\perp and J_\parallel by pressurization is ignored to simplify the analysis, and the contribution of the H2LLAF system is approximated with $\alpha M(P = 0 \text{ kbar})$. The quantity $(1 - \alpha)$ corresponds to the amount of the paramagnetic $S = 1/2$ spins, which are magnetically separated from the H2LLAF system. We used $g = 2.08$, referring to the result of the ESR of the powder sample by Deguchi *et al.*¹⁴ Equation (2) with $S = 1/2$, $g = 2.08$, and $\alpha = 0.50$ mol reproduces well the result of $M(P = 8 \text{ kbar})$ as shown in Fig. 1. This analytic result implies that 50% of spins behave paramagnetically and the residual 50% contribute to the dimer coupling in the ladder at $P = 8$ kbar.

Figure 2 shows the pressure dependence of the magnetic susceptibility (χ) of CuHpCl up to $P = 8$ kbar. At ambient pressure, an exponential-like drop below 6 K reflects the existence of the energy gap, and a broad hump around 7 K indicates the development of short-range ordering (SRO). Here the temperature is given in logarithmic scale. This result is quantitatively consistent with previous studies,^{7,8,10,13,14} and the overall temperature dependence of χ is reproduced by the series expansion for the $S = 1/2$ H2LLAF (Ref. 27) with $g = 2.08$, $J_\perp/k_B = -13.2$ K, and $J_\parallel/k_B = -2.4$ K. With increasing pressure, the development

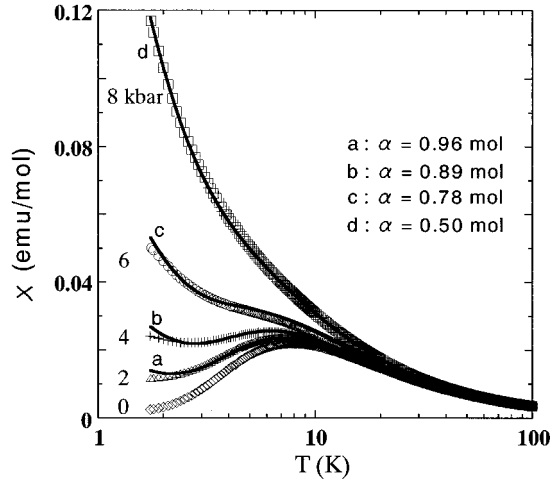


FIG. 2. Pressure dependence of magnetic susceptibility (χ) of CuHpCl up to $P=8$ kbar. The horizontal axis is logarithmically scaled. Four solid curves represent data obtained from Eq. (3) with $S=1/2$, $g=2.08$, and the following values of α : (a) $\alpha=0.96$ mol, (b) $\alpha=0.89$ mol, (c) $\alpha=0.78$ mol and (d) $\alpha=0.50$ mol.

of the paramagnetic component becomes obvious, similarly to the results for M , and tends to mask the intrinsic exponential-like drop of χ in the $S=1/2$ H2LLAF system. There is no trace of the $S=1/2$ H2LLAF system in the result for $P=8$ kbar.

Based on the same assumptions as those in the analysis of M , we analyze the results for χ in Fig. 2 with the following equation including the Curie law:

$$\chi(P) = \alpha\chi(P=0 \text{ kbar}) + (1 - \alpha) \frac{Ng^2\mu_B^2 S(S+1)}{3k_B T}, \quad (3)$$

where $g=2.08$ and $S=1/2$. As shown in Fig. 2, each result for χ under pressure is well reproduced with Eq. (3) using the following value of α : $\alpha=0.96$ mol ($P=2$ kbar), 0.89 mol (4 kbar), 0.78 mol (6 kbar), and 0.50 mol (8 kbar). The value of $\alpha=0.50$ mol at $P=8$ kbar, is quantitatively consistent with that in M .

In this section, we have analyzed the results for M and χ , based on the following two assumptions: (1) The free paramagnetic spins are induced by pressures, and (2) the relative changes of exchange interactions along the rung and leg in the ladder system are very small. The assumption (2) will be justified in the next subsection. However, the result for C_p will suggest that the induced paramagnetic spins are not completely free, but feel some magnetic exchange fields.

B. Thermal measurement

Figure 3 shows the pressure dependence of the magnetic heat capacity (C_p) of the present compound. At ambient pressure, the characteristic exponential behavior of C_p is seen below 4 K and the broad hump due to the SRO of the $S=1/2$ H2LLAF lies at around 5 K. The overall behavior of C_p can be well reproduced by the theoretical calculation

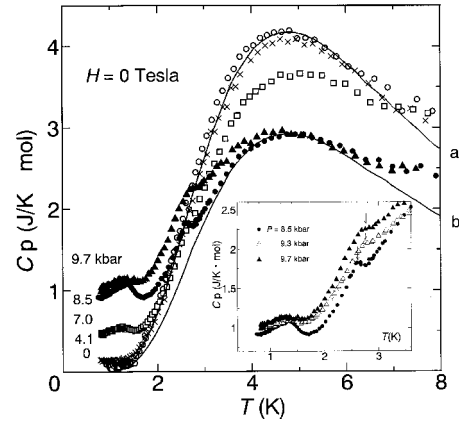


FIG. 3. Pressure dependence of heat capacity (C_p) of CuHpCl at zero magnetic field for $P=0$ kbar (\circ), 4.1 kbar (\times), 7.0 kbar (\square), 8.5 kbar (\bullet), and 9.7 kbar (\blacktriangle). (a) and (b) stand for the theoretical calculations of Gu *et al.* [Eq. (4)] for $\alpha=1.00$ and 0.70 mol. The inset figure shows the results below 3.6 K for $P \geq 8.5$ kbar.

of Gu *et al.* for the $S=1/2$ H2LLAF CuHpCl with $J_{\perp}/k_B = -13.2$ K and $J_{\parallel}/k_B = -2.4$ K (see the solid curve in Fig. 3), as reported earlier.^{10,19}

First, we focus on the pressure effect on the broad hump around 5 K. The application of pressure decreases the height of the broad hump, while its position is little changed. This suggests that exchange interactions along the rung and leg hardly change under pressure and the amount of spins (α) in the $S=1/2$ H2LLAF system decreases. This result justifies the assumption (2) in the analyses of M and χ in the previous subsection. Thus we estimate α at each pressure by analyzing the pressure dependence of the broad hump of C_p at around 5 K with the following equation:

$$C_p(P) = \alpha C_p(P=0 \text{ kbar}). \quad (4)$$

It is recalled here that the paramagnetic spins usually should not contribute to C_p at zero external field. The pressure dependence of α estimated by Eq. (4) is shown together with those estimated from M and χ in Fig. 4. The results for α from C_p , M , and χ are quantitatively consistent in the pres-

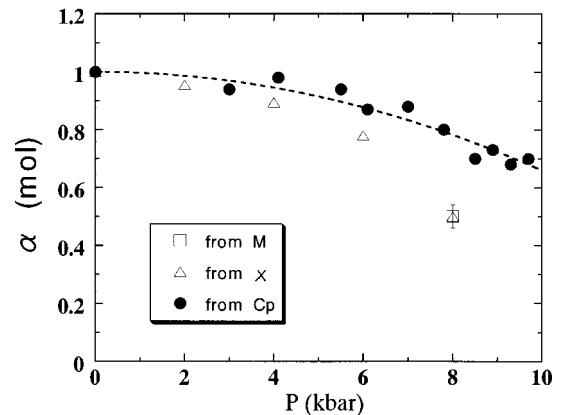


FIG. 4. Pressure dependence of α from M , χ , and C_p . The dotted curve expresses $\alpha(P) = 1 - 3.4 \times 10^{-3} P^2$.

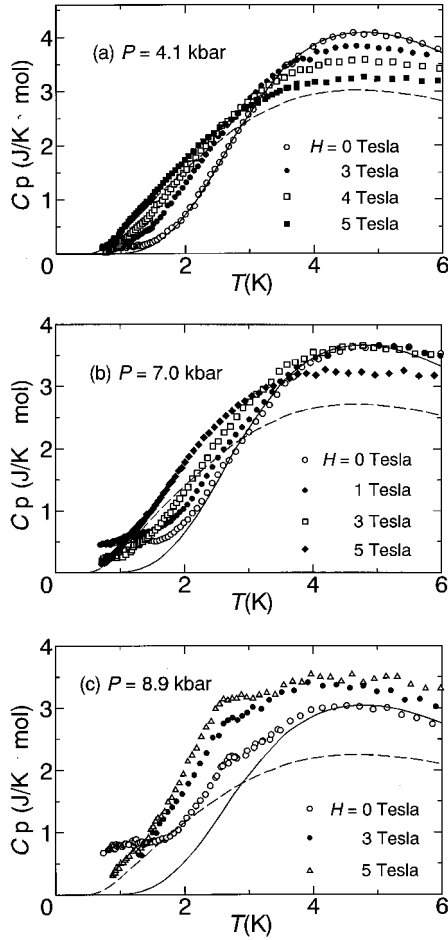


FIG. 5. Magnetic field dependence of C_p of CuHpCl for $P = 4.1$ kbar (a), 7.0 kbar (b), and 8.9 kbar (c). The solid and dashed curves show the theoretical calculations of Gu *et al.* [Eq. (4)] for $H = 0$ and 5 T with $\alpha = 0.98$ mol (a), 0.88 mol (b), and 0.73 mol (c), respectively.

sure region below 6 kbar. The estimation of α from C_p is, however, more reliable than those from M and χ . The analysis of the SRO hump in C_p directly estimates the amount of the spins in the H2LLAF system. On the other hand, the values of α estimated from M and χ seem to be rather ambiguous, because they are determined by the dominant paramagnetic component ($1 - \alpha$) under the assumption that the paramagnetic spins are free spins. Later we will see that they are not completely free and that at $P = 8$ kbar the paramagnetic component ($1 - \alpha$) has been overestimated in the analyses of M and χ . The pressure dependence of α from C_p is best fitted by $\alpha(P) = 1 - (3.4 \pm 0.2) \times 10^{-3} P^2$ in the pressure region up to 10 kbar.

Next, we mention the pressure effects on C_p below 3 K, where the change of Δ might be well seen. Two anomalies in C_p newly appear at around $T = 1.5$ K for $P \geq 7$ kbar and $T = 2.6$ K for $P \geq 8.5$ kbar, as shown in Fig. 3. We investigated the magnetic field effects on C_p to understand the character of the two anomalies. Figure 5 shows the magnetic field dependence of C_p at $P = 4.1$ kbar [Fig. 5(a)], 7.0 kbar [Fig. 5(b)], and 8.9 kbar [Fig. 5(c)]. The solid and dashed curves

stand for the theoretical calculations of Gu *et al.* at $H = 0$ and 5 T,¹⁹ respectively, using the same values of the exchange interactions. According to Eq. (4), the above theoretical data are multiplied by the following values: $\alpha = 0.98$ mol for $P = 4.1$ kbar, 0.88 mol for $P = 7.0$ kbar, and 0.73 mol for $P = 8.9$ kbar. At $P = 4.1$ kbar, the change of the low-temperature behavior from the exponential to the linear temperature dependences indicates the field-induced suppression of Δ , and this is qualitatively consistent with the results of the field dependence at ambient pressure, reported earlier.^{10,16,17} At $P = 7.0$ and 8.9 kbar, a broad anomaly appears at around 1.5 K at zero magnetic field, but it tends to be masked by the above changes of the initial slope due to the suppression of Δ under the magnetic fields. This magnetic field effect is essentially different from that of the field-induced magnetic order reported at ambient pressure.^{10,16,17} This anomaly is probably not related to any magnetic long-range ordering, and its origin will be mentioned later. Furthermore, at $P = 8.9$ kbar, one more anomaly appears at around $T = 2.6$ K. This anomaly survives under large magnetic fields, as shown in Fig. 3(c), and shows a magnetic field dependence different from that seen in the anomaly at around 1.5 K. We consider that it reflects some rigid magnetic ordering and will also be discussed later.

In order to analyze the above two anomalies in more detail, we need to separate C_p into the H2LLAF component C_p (ladder) and the rest $\Delta C_p = C_p - C_p$ (ladder). As for C_p (ladder), the theoretical calculations of Gu *et al.* are used for each magnetic field, as shown in Fig. 5. Figure 6 shows ΔC_p under $H = 0$ and 5 T for $P = 4.1$ kbar [Fig. 6(a)], 7.0 kbar [Fig. 6(b)], and 8.9 kbar [Fig. 6(c)]. The solid and dashed curves show the Schottky-type heat capacity (SHC) for a two-level model, which is equivalent to the free-spin model of $S = 1/2$ under some magnetic fields [see Fig. 7(a)]. At first, even at $P = 4.1$ kbar, we notice the existence of a small ΔC_p at around 1 K even at zero magnetic field. Applying $H = 5$ T, the anomaly of ΔC_p shifts toward higher temperatures, maintaining about the same magnitude. This is a characteristic of the two-level SHC system and surely originates from the existence of the paramagnetic component, as mentioned in the results for M and χ . The results for ΔC_p for $H = 0$ and 5 T at $P = 4.1$ kbar are reproduced by the SHC model for the $S = 1/2$ spins of 0.06 mol under the assumed magnetic fields $H' = 1.0 \pm 0.2$ and 5.5 ± 0.5 T, respectively. At zero magnetic field, however, the heat capacity due to the free spins should be zero, and there is a deviation of about 1 T between the actual external field (H) and the assumed magnetic field (H') [see Fig. 7(b)]. These results suggest that the pressure-induced paramagnetic spins feel an exchange field ($H_{\text{int}} = H' - H$). The similar result has also been reported in $\text{Sr}(\text{Cu}_{1-x}\text{Zn}_x)_2\text{O}_3$, where Azuma *et al.* reported that the impurity-induced paramagnetism obeys the Curie-Weiss law with a small negative Weiss constant (≈ -2 K).⁵ We suppose that the exchange field of CuHpCl originates from the magnetic correlation between the paramagnetic spins and spins on the H2LLAF system. The behavior seen at $P = 4.1$ kbar becomes more pronounced at $P = 7.0$ and 8.9 kbar as seen in Figs. 6(b) and 6(c). The amounts of the induced paramagnetic $S = 1/2$ spins at $P = 7.0$ and 8.9 kbar are estimated to be

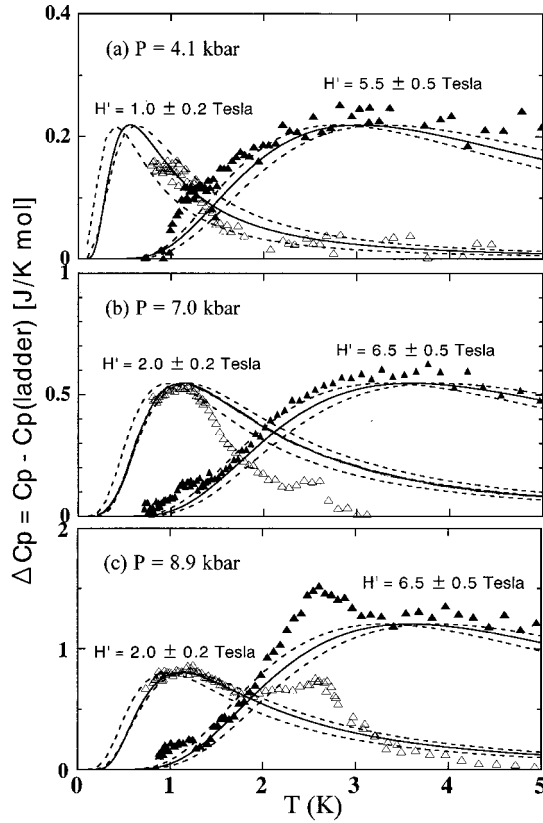


FIG. 6. Pressure-induced heat capacity $\Delta C_p = C_p - C_p$ (ladder) under $H=0$ T (Δ) and 5 T (\blacktriangle) for $P=4.1$ kbar (a), 7.0 kbar (b), and 8.9 kbar (c). The solid and dashed curves stand for the Schottky-type heat capacities under the assumed magnetic fields H' with the following amount of $S=1/2$ spins: (a) 0.06 mol for $H=0$ and 5 T, (b) 0.15 mol for $H=0$ and 5 T, and (c) 0.22 mol for $H=0$ T and 0.33 mol for $H=5$ T.

0.15 and 0.22 mol, which are close to the value of $(1 - \alpha)$ estimated in Fig. 5 for each pressure. This paramagnetic anomaly in ΔC_p shifts toward higher temperatures with increasing pressure, and this indicates that the H_{int} is enhanced by pressure. The magnetic correlation between the paramagnetic spins and spins of the ladder also seems to be enhanced by pressures. Figure 8 shows the pressure dependence of H_{int} , which has been estimated for both $H=0$ and 5 T. The value of H_{int} at $H=5$ T is slightly larger than that at $H=0$ T, but qualitatively shows the similar pressure dependence. The H_{int} seems to saturate above 7 kbar. The magnitude of saturated H_{int} above 7 kbar ($\mu_B H_{\text{int}}/k_B \sim 1.0-1.3$ K) is as much as half of the exchange interaction along the leg of the ladder. The deviation between the values of α estimated from C_p and those from M and χ (Fig. 4) may come from overestimating the paramagnetic component $(1 - \alpha)$ due to ignoring the effect of the exchange field in the latter cases.

Next, we consider the second anomaly of C_p at around 2.6 K, which appears for $P \geq 8.5$ kbar. At $P=8.9$ kbar, we can extract the anomaly at around 2.6 K by subtracting the paramagnetic SHC from ΔC_p , as shown in Fig. 6(c). The estimated magnetic entropy for the second anomaly at $P=8.9$ kbar is 9.4×10^{-2} J/K mol, which is 1.6% of the total

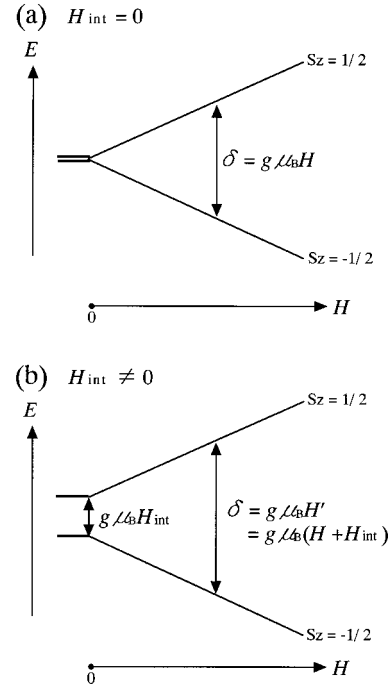


FIG. 7. (a) Energy level (E) of the free paramagnetic spin with $S=1/2$ under magnetic field (H). The energy deviation between two energy levels of $S_z=1/2, -1/2$ is shown as $\delta = g\mu_B H$. (b) Energy level of the paramagnetic spin with $S=1/2$ feeling the exchange field (H_{int}). The assumed magnetic field H' is $H' = H + H_{\text{int}}$. Even at $H=0$, there is the energy deviation of $g\mu_B H_{\text{int}}$.

entropy for $S=1/2$. This anomaly survives even under $H=5$ T, at around the same temperature of 2.6 K. We assume that it is probably due to the magnetic long-range ordering of the H2LLAF system.

Figure 9 shows the temperature dependences of χ' , C_p , and ΔC_p under zero field at $P=9.7$ kbar, which is the maximum pressure in the present series of experiments. From the analyses of C_p and ΔC_p , the amount of the induced paramagnetic spins at $P=9.7$ kbar is 0.30 mol, and the entropy for the second anomaly at around 2.6 K is 9.8×10^{-2} J/K mol (1.7% of the total entropy for $S=1/2$). However, the χ' has no anomaly at around 2.6 K and shows a

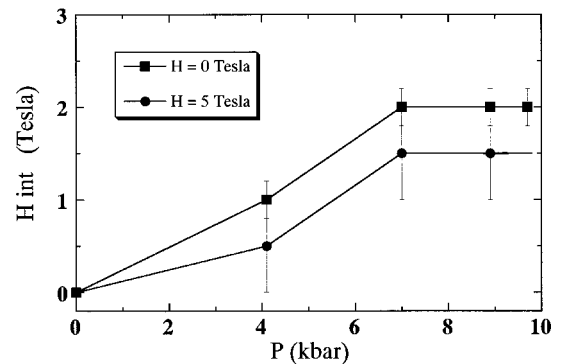


FIG. 8. Pressure dependence of exchange field H_{int} under external fields $H=0$ and 5 T. The solid lines are guides for the eye. The exchange field seems to saturate above $P=7$ kbar.

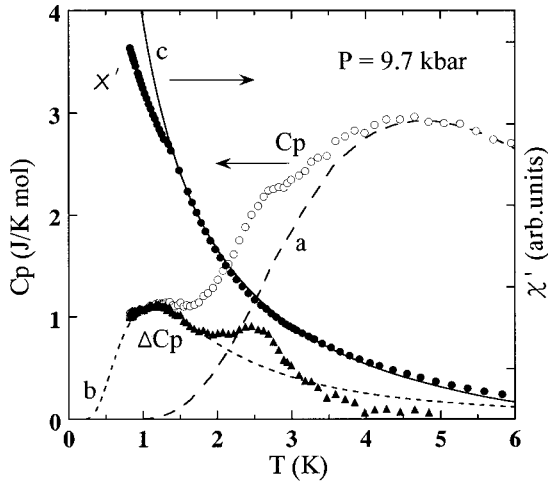


FIG. 9. Temperature dependences of C_p (\circ), ΔC_p (\blacktriangle), and χ' (\bullet) under zero magnetic field at $P=9.7$ kbar. The dashed curve (a) stands for the theoretical calculations of Gu *et al.* [Eq. (4)] for $\alpha=0.70$ mol. The dotted curve (b) is the Schottky-type heat capacity for the $S=1/2$ spins of 0.30 mol and $H'=2$ T. The solid curve (c) shows the temperature dependence of $1/T$, corresponding to Curie law.

temperature dependence proportional to $1/T$, as seen in the solid curve (c). On the other hand, the χ' slightly deviates from the Curie law at around 1.4 K, where the paramagnetic anomaly of C_p appears supposedly due to an antiferromagnetic exchange field H_{int} .

Here we define the magnetic ordering temperature T_N , at which the second anomaly of C_p mentioned above appears, and give its pressure dependence in Fig. 10. Magnetic order appears above 8.5 kbar, where paramagnetic spins of more than 0.2 mol are induced and the exchange field saturates. The pressurization decreases the number of the interaction paths via the increase of the paramagnetic spins in the H2LLAF system, but simultaneously modulates the staggered moments in the H2LLAF system. Therefore T_N may show no significant enhancement by pressures ($P \geq 8.5$ kbar).

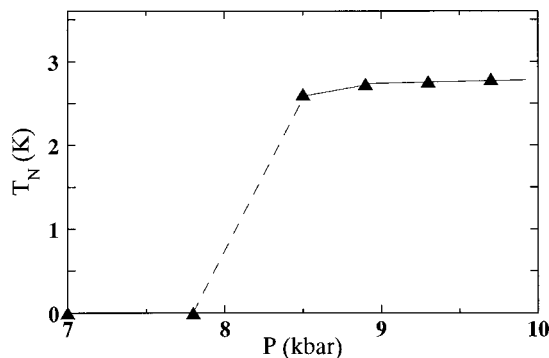


FIG. 10. Pressure dependence of magnetic ordering temperature T_N , which appears above 8.5 kbar and is slightly enhanced by the further pressure. The solid and dashed lines are guides for the eye.

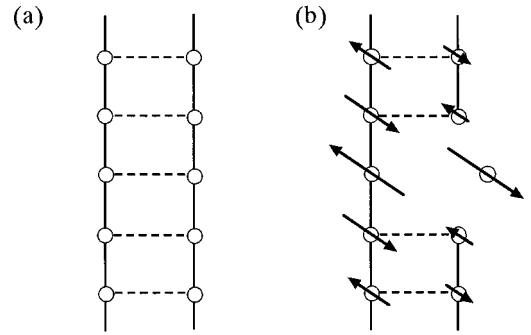


FIG. 11. (a) A schematic view of the $S=1/2$ H2LLAF system. The open circle stands for the spin $S=1/2$. The solid and dashed lines represent the interactions along the leg and rung, respectively. (b) A possible view of CuHpCl under pressures. The spatial pattern of the staggered magnetization in the two-leg ladder system and the paramagnetic spin magnetically separated from the two-leg ladder system are schematically drawn.

IV. DISCUSSION

In the Zn-doped system of the $S=1/2$ H2LLAF SrCu_2O_3 [$\text{Sr}(\text{Cu}_{1-x}\text{Zn}_x)_2\text{O}_3$], the increase of the paramagnetic susceptibility with increasing x has been observed and, furthermore, antiferromagnetic order has been detected in the doped region of $0.01 < x < 0.08$.⁵ Fukuyama *et al.* have theoretically explained that the magnetic order is triggered by the modulation of the staggered moment induced by the local randomness.¹⁸

Our experimental results of the pressure effects in CuHpCl are very similar to the above-mentioned doping effects in SrCu_2O_3 . We propose the following model to explain the pressure effects on CuHpCl accompanying the pressure-induced paramagnetic behavior and a magnetic ordering, referring to the above model of Fukuyama *et al.*¹⁸. At first, pressurization may apply a local strain to the ladder of CuHpCl and destroy the dimer coupling, inducing the paramagnetic spins magnetically separated from the H2LLAF system (see Fig. 11). The separated paramagnetic spins are not completely free and have a magnetic correlation with the H2LLAF system. The defects in the H2LLAF system bring about a modulation of the staggered moment, whose development triggers magnetic order in the H2LLAF system under high pressure. But pressurization also decreases the interaction paths and, therefore, the magnetic ordering temperature T_N may be not significantly enhanced by further pressurization. The magnetically separated paramagnetic spins are not directly related to the magnetic order, and paramagnetism and long-range order of the H2LLAF system probably coexist below T_N .

In the study of doping effects in CuHpCl with Zn^{2+} impurities, the increase of the paramagnetic susceptibility with Zn^{2+} concentration (up to 11.7%) has been observed by Deguchi *et al.*, but no anomaly of magnetic order has been observed yet.¹⁴ The doped state with the Zn^{2+} concentration of about 10% corresponds to a pressurized state under $P=5-6$ kbar, where magnetic order has not been observed.

Finally we have checked the reversibility of the sample for pressurization by a powdered x-ray diffraction experi-

ment, as well as measuring M , χ , and C_p , again after releasing the pressure down to ambient pressure. The reversible results have been obtained in the considered pressure region. We have also been trying to do a structural analysis of CuHpCl under pressure to get structural information about the magnetically separated paramagnetic spins, but the analysis is very difficult due to the low structural symmetry of CuHpCl.

V. CONCLUSION

The pressure effects on an $S = 1/2$ Heisenberg two-leg ladder antiferromagnet CuHpCl have been investigated through magnetic and thermal measurements up to 10 kbar. The exchange interactions in the ladder hardly change under pressure. But we observed that the pressurization induces the paramagnetic spins and magnetic ordering in the H2LLAF system. This magnetic order is the first pressure-induced one observed in the quantum spin system with the energy gap. The amount of induced paramagnetic spins increases almost in accordance with the square of pressure. The induced paramagnetic spins are not completely free, but probably have the magnetic correlation with the H2LLAF system. Furthermore, the anomaly of the magnetic heat capacity appears at around 2.6 K at $P \geq 8.5$ kbar, where the paramagnetic spins of more than 20% are induced and they feel the exchange

field of about 1 K. We consider that it is relevant to the magnetic order in the H2LLAF system. These pressure effects are similar to the result of nonmagnetic impurity effects in SrCu_2O_3 . We assume that applying pressure in CuHpCl locally destroys the dimer coupling and produces paramagnetic spins, producing local defects in the ladder just as in the case of doping effects. The local defects induce a modulation of the staggered moment in the ladder, whose development may trigger magnetic order in the H2LLAF system under high pressures. The magnetic long-range order of the H2LLAF system and paramagnetism are slightly dependent, but coexist below the magnetic ordering temperature. Analysis of the data of the crystal structure under pressure is currently underway.

ACKNOWLEDGMENTS

We would like to thank M. Yoshihiro (Kyushu Institute of Technology) and S. Momota (Kyushu University) for their indispensable support in our experiments under pressure. We also would like to thank Dr. M. Žukovič for a careful reading of the manuscript. This work was supported in part by a Grant-in-Aid for Scientific Research (A) and a Grant-in-Aid for Scientific Research on Priority Areas (B) of Molecular Conductors and Magnets from the Ministry of Education, Science, Sports and Culture, Japan.

-
- ¹See, for example, F. D. M. Haldane, *Phys. Rev. Lett.* **50**, 1153 (1983); K. Katsumata, H. Hori, T. Takeuchi, M. Date, A. Yamagishi, and J. P. Renard, *ibid.* **63**, 86 (1989); Y. Ajiro, T. Goto, H. Kikuchi, T. Sakakibara, and T. Inami, *ibid.* **63**, 1424 (1989).
- ²See, for example, M. Hase, I. Terasaki, and K. Uchinokura, *Phys. Rev. Lett.* **70**, 3651 (1993).
- ³M. Azuma, Z. Hori, M. Takano, K. Ishida, and Y. Kitaoka, *Phys. Rev. Lett.* **73**, 3463 (1994).
- ⁴K. Ishida, Y. Fujishiro, M. Takano, M. Nohara, and H. Takagi, *Phys. Rev. B* **55**, 8658 (1997).
- ⁵M. Azuma, Y. Fujishiro, M. Takano, M. Nohara, and H. Takagi, *Phys. Rev. B* **55**, 8658 (1997).
- ⁶B. Chiari, O. Piovesana, T. Tarantelli, and P. F. Zanazzi, *Inorg. Chem.* **29**, 1172 (1990).
- ⁷P. R. Hammar and D. H. Reich, *J. Appl. Phys.* **79**, 5392 (1996).
- ⁸G. Chaboussant, P. A. Crowell, L. P. Levy, O. Piovesana, A. Madouri, and D. Mailly, *Phys. Rev. B* **55**, 3046 (1997).
- ⁹G. Chaboussant, H.-H. Julien, Y. Fagot-Revurat, L. P. Levy, C. Berthier, M. Horvatic, and O. Piovesana, *Phys. Rev. Lett.* **79**, 925 (1997).
- ¹⁰P. R. Hammar, D. H. Reich, C. Broholm, and F. Trouw, *Phys. Rev. B* **57**, 7846 (1998).
- ¹¹G. Chaboussant, H.-H. Julien, Y. Fagot-Revurat, M. Hanson, L. P. Levy, C. Berthier, M. Horvatic, and O. Piovesana, *Eur. Phys. J. B* **6**, 167 (1998).
- ¹²M. Chiba, T. Fukui, Y. Ajiro, M. Hagiwara, T. Goto, and T. Kubo, *Physica B* **246–247**, 576 (1998).
- ¹³M. Hagiwara, Y. Narumi, K. Kindo, T. Nishida, M. Kaburagi, and T. Tonegawa, *Physica B* **246–247**, 234 (1998).
- ¹⁴H. Deguchi, S. Sumoto, S. Takagi, M. Mito, T. Kawae, K. Takeda, H. Nojiri, T. Sakon, and M. Motokawa, *J. Phys. Soc. Jpn.* **67**, 3707 (1998).
- ¹⁵H. Ohta, T. Tanaka, S. Okubo, S. Kimura, H. Kikuchi, and H. Nagaosa, *J. Phys. Soc. Jpn.* **68**, 732 (1999).
- ¹⁶R. Calemczuk, J. Riera, D. Poiblan, J.-P. Boucher, G. Chaboussant, L. P. Levy, and O. Piovesana, *Eur. Phys. J. B* **7**, 171 (1999).
- ¹⁷M. Hagiwara, H. A. Katori, U. Schollwock, and H.-J. Mikeska, *Phys. Rev. B* **62**, 1051 (2000).
- ¹⁸H. Fukuyama, Naoto, M. Saito, and T. Tanimoto, *J. Phys. Soc. Jpn.* **65**, 2377 (1996).
- ¹⁹Q. Gu, D-Ke Yu, and J-L. Shen, *Phys. Rev. B* **60**, 3009 (1999).
- ²⁰S. Wessel and S. Haas, *Phys. Rev. B* **62**, 316 (2000).
- ²¹Z. Honda, K. Katsumata, H. A. Katori, K. Yamada, T. Ohishi, T. Manabe, and M. Yamashita, *J. Phys.: Condens. Matter* **9**, L83 (1997).
- ²²Z. Honda, H. Asakawa, and K. Katsumata, *Phys. Rev. Lett.* **81**, 2566 (1998).
- ²³Y. Hosokoshi, M. Tamura, and M. Kinoshita, *Mol. Cryst. Liq. Cryst. Sci. Technol., Sect. A* **306**, 423 (1997).
- ²⁴K. Takeda, M. Wada, M. Inoue, and T. Haseda, *Jpn. J. Appl. Phys., Part 1* **26**, 947 (1987).
- ²⁵K. Takeda, K. Konishi, M. Tamura, and M. Kinoshita, *Phys. Rev. B* **53**, 3374 (1996).
- ²⁶A. Eiling and J. S. Schilling, *J. Phys. F* **11**, 623 (1981).
- ²⁷Z. Weihong, R. R. P. Singh, and J. Oitmaa, *Phys. Rev. B* **55**, 8052 (1997).